

Tunable absorption spectrum splitting in a pulse-driven three-level system

Jiawei Wang,¹ Anthony Gullo,¹ Kavya Velmurugan,² and Herbert F Fotso^{1,*}

¹*Department of Physics, University at Buffalo SUNY, Buffalo, New York 14260, USA*

²*College of Computing, Georgia Institute of Technology, Atlanta, Georgia 30332, USA*

When a two-level system is driven on resonance by a strong incident field, its emission spectrum is characterized by the well-known Mollow triplet. If the absorption from the excited state, in this continuously driven two-level system, to a third, higher energy level, is probed by a weak field, the resulting absorption spectrum features the Autler-Townes doublet with two peaks separated by the Rabi frequency of the strong driving field. It has been shown that when the two-level system is instead driven by a periodic pulse sequence, the emission spectrum obtained has similarities with the Mollow triplet even though the system is only driven during the short application time of the pulses and is allowed to evolve freely between pulses. Here, we evaluate the absorption spectrum of the three-level system in the ladder/cascade configuration when the bottom two levels are driven by a periodic pulse sequence while the transition between the middle and the highest level is probed by a weak field. The absorption spectrum displays similarities with the Autler-Townes doublet with frequency separation between the main peaks defined by the inter-pulse delay. In addition, this spectrum shows little dependence on the pulse carrier frequency. These results demonstrate the capacity to modulate the absorption spectrum of a three-level system with experimentally achievable pulse protocols.

I. INTRODUCTION

Driving quantum emitters with external control fields can drastically modify their spectral properties and, importantly, enable novel applications. For a two-level system, a strong resonant field produces the resonance fluorescence spectrum characterized by the Mollow triplet with a central peak at the emitter's frequency and two satellite peaks shifted by the Rabi frequency of the driving field on either side of the central peak [1–3]. Various studies have recently considered the possibility of replacing the continuous resonant driving field with a variety of pulse sequences and revealed a great deal of tunability in the resulting spectral properties [4–7]. For example, it was found that a periodic sequence of π_x pulses applied on initially different or even noisy two-level systems can enhance the efficiency of Hong-Ou-Mandel two-photon interference experiments [8, 9]. Similarly, it has been shown that the same sequence of π_x pulses suppresses inhomogeneous broadening in the emission or absorption spectrum of a heterogeneous ensemble of two-level systems. The protocol refocuses the absorption spectrum of an ensemble of nitrogen vacancy centers and has thus been shown to restore the $1/T_2$ sensitivity when such an ensemble is used for magnetometry [10, 11].

Beyond the two-level systems, when a third energy level is included, for a three-level system e.g. in the Λ configuration, a driving field can give rise to electromagnetically induced transparency [12, 13] with prominent applications in quantum memories [14–18]. The parent phenomenon, the Autler-Townes splitting, is observed for a strongly driven system and has also been implemented as a protocol for quantum memories [19–23]. Given the

mentioned effects of pulse sequences on two-level systems, it is then natural to investigate their effects on three-level systems and to explore potential advantages that they can provide in this context. In the present paper, we study the absorption spectrum of the three-level system in the ladder or cascade configuration when the transition between the bottom two levels is driven by a periodic pulse sequence while the transition between the middle and the highest energy level is probed with a weak field. We find that the resulting absorption spectrum displays similarities with the Autler-Townes doublet with separation between the main peaks defined by the inverse of the inter-pulse delay. In addition, this spectrum shows little dependence on the pulse carrier frequency. These results demonstrate a flexible capacity to modulate the absorption spectrum of a three-level system with achievable pulse protocols, highlighting alternative implementations of quantum memories in these systems.

The rest of the paper is structured as follows. In section II, we introduce the model of the three-level system in the ladder configuration under the influence of the pulse sequence and the probing field. In this section, we also discuss the algorithm for our numerical solution of the relevant master equation governing the time evolution of the density matrix operator of the three-level system. In section III, we present the results of the spectrum and its dependence on the system and drive parameters before concluding the paper in section IV.

II. MODEL AND NUMERICAL SOLUTION

We consider a three-level system in the ladder configuration with energy levels $|1\rangle$, $|2\rangle$, and $|3\rangle$ with respective energies, E_1 , E_2 and E_3 with $E_1 < E_2 < E_3$. This

* hffotso@buffalo.edu

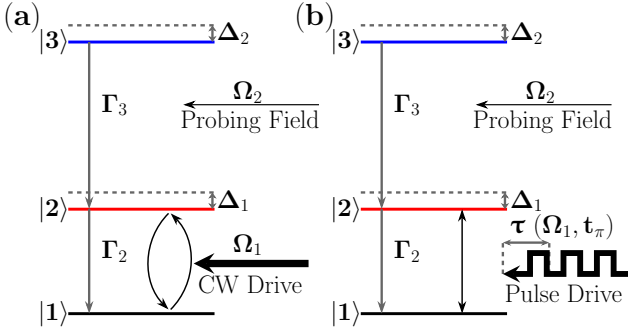


FIG. 1. Schematic representation of a three-level system in a ladder/cascade configuration. The Autler-Townes splitting is observed in the absorption from the first excited state ($|2\rangle$) to the top excited state ($|3\rangle$), probed by a weak field of Rabi frequency Ω_2 , when the bottom transition ($|1\rangle \leftrightarrow |2\rangle$) is driven continuously on resonance by a strong continuous drive of Rabi frequency Ω_1 (a). Here, we will evaluate the ($|2\rangle \leftrightarrow |3\rangle$) absorption spectrum when the ($|1\rangle \leftrightarrow |2\rangle$) is driven by a periodic sequence of π pulses produced by periodically applying on the transition a field of Rabi frequency Ω_1 for time $t_\pi = \pi/\Omega_1$ (b).

system is placed in a bosonic bath of photons to which it is coupled. In the usual formulation of the Autler-Townes effect, (Fig. 1 (a)) the $|1\rangle \leftrightarrow |2\rangle$ transition is driven strongly while the $|2\rangle \leftrightarrow |3\rangle$ transition is gauged by a weak probing field. The measured absorption spectrum displays, when the driving field is resonant with the $|1\rangle \leftrightarrow |2\rangle$ transition, two symmetric peaks around the transition frequency that are separated by the Rabi frequency (Ω_1) of the driving field. This splitting is due to the dressed states, around the ground and the excited states, that are formed in the resonantly driven two-level system. A finite detuning (Δ_1) between the driving field frequency ω_1 and the transition frequency leads to an asymmetry in the position and the magnitude of the peaks.

Here, we consider the situation where the $|1\rangle \leftrightarrow |2\rangle$ transition is instead driven by a periodic sequence of finite width π_x pulses (Fig. 1 (b)). To this end, we apply a driving field with a time dependent Rabi frequency $\Omega_1(t)$ such that, $\Omega_1(t) = \Omega_1$ during the pulse and is zero otherwise. Similarly to the conventional Autler-Townes splitting setup, the probing field, at frequency $\omega = E_3 - E_2 + \Delta_2$, with a Rabi frequency $\Omega_2 \ll \Omega_1$, is applied at all times. The driving field is finite for time $t_\pi = \pi/\Omega_1$. The relaxation rate from state $|2\rangle$ to state $|1\rangle$ is Γ_2 while the relaxation rate from state $|3\rangle$ to state $|2\rangle$ is Γ_3 , and there is no direct transition allowed between states $|1\rangle$ and $|3\rangle$. We set $\Gamma_2 = 2$ and we measure our energy and time in units of Γ_2 and $1/\Gamma_2$ respectively.

The Hamiltonian describing the 3-level system in the radiation field, in the presence of the driving and probing field is made of five parts and can be written as:

$$H = H_A + H_F + H_{AF} + H_d(t) + H_p(t). \quad (1)$$

Where H_A , H_F , and H_{AF} are, respectively, the Hamiltonian describing the atom, the field modes and the coupling between the atom and the field mode. $H_d(t)$ corresponds to the driving field on the $|1\rangle \leftrightarrow |2\rangle$ transition. While $H_p(t)$ describes the probing field coupled to the $|2\rangle \leftrightarrow |3\rangle$ transition.

The driving field is treated at a semi-classical level which is consistent with driving the emitter with a coherent field [3].

To characterize the time evolution of the system, we will use the density matrix operator of the 3-level system when the bosonic degrees of freedom are integrated out of the problem. This density matrix operator of the 3-level system is given by

$$\begin{aligned} \rho = & \rho_{11}|1\rangle\langle 1| + \rho_{22}|2\rangle\langle 2| + \rho_{33}|3\rangle\langle 3| \\ & + \rho_{21}|2\rangle\langle 1| + \rho_{12}|1\rangle\langle 2| + \rho_{32}|3\rangle\langle 2| \\ & + \rho_{23}|2\rangle\langle 3| + \rho_{31}|3\rangle\langle 1| + \rho_{13}|1\rangle\langle 3| \end{aligned} \quad (2)$$

In general, ρ_{ij} 's for $i, j = 1, 2, 3$ are complex numbers. However, as a result of hermiticity, ρ_{ii} 's for $i = 1, 2, 3$ are real and only 6 matrix elements of the density matrix operator are independent. Furthermore, we have the identity $\rho_{11} + \rho_{22} + \rho_{33} = 1$.

One can use the Lindblad equation or the independent-rate approach to obtain the equations of motion due to the different terms of the Hamiltonian. The resulting master equations, stated below term by term, characterize the time evolution of the density matrix operator [3, 24].

$$\dot{\rho}_{11} = \Gamma_2\rho_{22} - i\frac{\Omega_1}{2}\rho_{21} + i\frac{\Omega_1}{2}\rho_{21}^* \quad (3)$$

$$\begin{aligned} \dot{\rho}_{22} = & -\Gamma_2\rho_{22} + \Gamma_3\rho_{33} + i\frac{\Omega_1}{2}\rho_{21} \\ & - i\frac{\Omega_1}{2}\rho_{21}^* - i\frac{\Omega_2}{2}\rho_{32} + i\frac{\Omega_2}{2}\rho_{32}^* \end{aligned} \quad (4)$$

$$\dot{\rho}_{33} = -\Gamma_3\rho_{33} + i\frac{\Omega_2}{2}\rho_{32} - i\frac{\Omega_2}{2}\rho_{32}^* \quad (5)$$

$$\begin{aligned} \dot{\rho}_{21} = & -i\frac{\Omega_1}{2}\rho_{11} + i\frac{\Omega_1}{2}\rho_{22} \\ & + \left[i\Delta_1 - \frac{1}{2}\Gamma_2 \right] \rho_{21} - i\frac{\Omega_2}{2}\rho_{31} \end{aligned} \quad (6)$$

$$\begin{aligned} \dot{\rho}_{32} = & -i\frac{\Omega_2}{2}\rho_{22} + i\frac{\Omega_2}{2}\rho_{33} \\ & + \left[i\Delta_2 - \frac{1}{2}\Gamma_{32} \right] \rho_{32} + i\frac{\Omega_1}{2}\rho_{31} \end{aligned} \quad (7)$$

$$\begin{aligned} \dot{\rho}_{31} = & -i\frac{\Omega_2}{2}\rho_{21} + i\frac{\Omega_1}{2}\rho_{32} \\ & + \left[i(\Delta_1 + \Delta_2) - \frac{1}{2}\Gamma_3 \right] \rho_{31} \end{aligned} \quad (8)$$

Here factors of $e^{i\omega_1 t}$, $e^{i\omega t}$, and $e^{i(\omega_1 + \omega)t}$ have been included in ρ_{21} , ρ_{32} and ρ_{31} respectively. Note also that ρ_{12} and ρ_{23} have respectively been replaced in these equations by ρ_{21}^* and ρ_{32}^* , using the above-mentioned properties of the density matrix operator. Γ_2 and Γ_3 are the

transition rates between the $|2\rangle$ and the $|1\rangle$ states, and between the $|3\rangle$ and the $|2\rangle$ states respectively. In addition, we have introduced the parameter $\Gamma_{32} = \Gamma_3 + \Gamma_2$. For a continuously driven $|1\rangle \leftrightarrow |2\rangle$ transition, a steady expression for the occupation of the highest energy level has been derived [24]. For the pulse driven system, however, the solution becomes untractable and we resort to a numerical solution.

At time $t = 0$, the system is prepared in the state $|2\rangle$. All matrix elements are set to zero except for $\rho_{22} = 1$. The transition between the lower energy level $|1\rangle$ and the intermediate energy level $|2\rangle$ is then driven periodically with inter-pulse delay τ , and pulses applied by a field of Rabi frequency Ω_1 , that is applied for a time π/Ω_1 amounting to a finite width π -pulse. The weak probing field, with Rabi frequency $\Omega_2 (\ll \Omega_1)$ is applied at all times on the transition between the intermediate energy level $|2\rangle$ and the upper energy level $|3\rangle$.

We integrate these differential equations iteratively starting from the initial conditions for the density matrix operator $\rho(t_0 = 0)$ and calculate $\rho(t_0 + \delta t)$, $\rho(t_0 + 2\delta t)$... up to $\rho(t_0 + N_t \delta t) = \rho(t_{max})$. Where $t_{max} = N_t \delta t$ and N_t is the number of time steps of width δt . The time step δt is chosen such that the discretization error is negligible. The time evolution of the density matrix characterized by equations (3 - 8), is carried out for frequencies ω of the weak probing field, covering a range of values of Δ_2 from $\omega_{min} = -40$ to $\omega_{max} = 40$ outside of which there is negligible spectral weight. For each probing field frequency, we evolve the system up to a maximum time when the system has reached the steady state. The steady state here is identified by tracking the time evolution of the density matrix operator, particularly the occupation number of the highest excited state, ρ_{33} , and confirming that it is no longer changing appreciably.

The absorption spectrum of interest is then defined by the occupation of the highest excited state, ρ_{33} , in this steady state, for varying values ω of the probing field frequency.

III. RESULTS

We start by assessing the realization of the steady state in our pulse-driven system. Fig. 2 shows $\rho_{33}(t)$, the population of the highest excited state ($|3\rangle$) as a function of time, when the ($|1\rangle \leftrightarrow |2\rangle$) transition is driven by a periodic sequence of π pulses with period $\tau = 0.3$. Here, the pulses are due to a driving field of Rabi frequency $\Omega_1 = 50$ that is applied for time $t_\pi = \pi/\Omega_1$. $\rho_{33}(t)$ is shown for $\omega = 0$ (solid green line), $\pi/2\tau$ (dashed blue line), $3\pi/2\tau$ (dashed red line). The figure clearly shows that after an initial non-trivial transient, the system settles into a steady state where the population for any frequency does not show any non-trivial change as a function of time. The rest of the data that we present throughout this paper corresponds to this steady state. Here and in what follows, we choose $\Gamma_3 = 0.2$ and

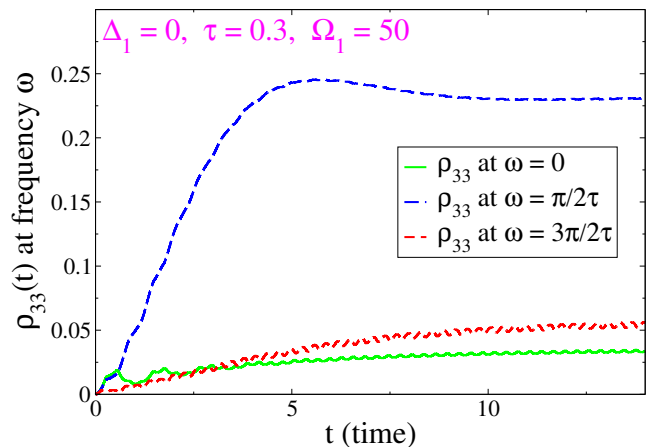


FIG. 2. Population of the second excited state ($|3\rangle$) as a function of time, $\rho_{33}(t)$, when the ($|1\rangle \leftrightarrow |2\rangle$) transition is driven by a periodic sequence of π pulses with period $\tau = 0.3$. The pulse carrier frequency is resonant with the transition, $\Delta_1 = 0$, and the pulses are due to a driving field of Rabi frequency $\Omega_1 = 50$ that is periodically applied for time $t_\pi = \pi/\Omega_1$. $\rho_{33}(t)$ is shown for $\omega = 0$ (solid green line), $\pi/2\tau$ (dashed blue line) and $3\pi/2\tau$ (dashed red line).

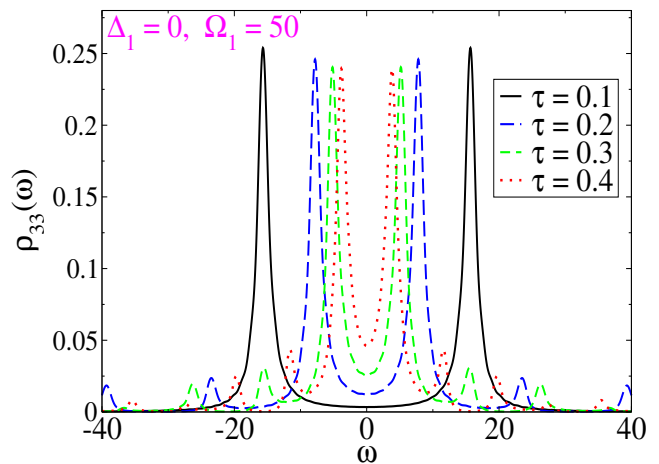


FIG. 3. Population of the second excited state or absorption spectrum of the ($|2\rangle \leftrightarrow |3\rangle$) transition when the ($|1\rangle \leftrightarrow |2\rangle$) is driven by a periodic sequence of π pulses with period τ the pulse is due to a driving field of Rabi frequency $\Omega_1 = 50$ that is applied for time $t_\pi = \pi/\Omega_1$. Absorption spectrum shown for detuning $\Delta_1 = 0$ under pulse sequences of different periods: $\tau = 0.1$ (black solid line), $\tau = 0.2$ (dashed blue line), $\tau = 0.3$ (dashed green line), $\tau = 0.4$ (dotted red line).

$\Omega_2 = 1.0$ but we note that the same lineshape is obtained for $\Omega_2 = 0.1$ with the only difference that the peaks in the absorption spectrum have higher magnitudes for larger Ω_2 .

Fig. 3 shows, for detuning $\Delta_1 = 0$, the absorption spectrum of the ($|2\rangle \leftrightarrow |3\rangle$) transition, or the population of the highest excited state as a function of frequency, when the ($|1\rangle \leftrightarrow |2\rangle$) is driven by a periodic sequence of π pulses with different values of the period τ . The pulse

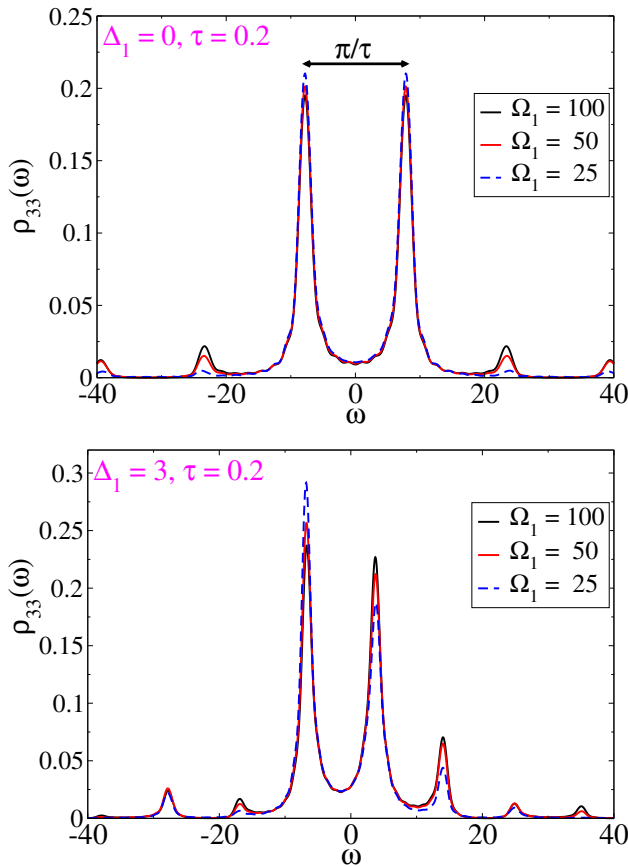


FIG. 4. Population of the second excited state or absorption spectrum of the ($|2\rangle \leftrightarrow |3\rangle$) transition when the ($|1\rangle \leftrightarrow |2\rangle$) is driven by a periodic sequence of π pulses with period τ the pulse is due to a driving field of Rabi frequency $\Omega_1 = 100$ (solid black line), $\Omega_1 = 50$ (solid red line), $\Omega_1 = 25$ (dashed blue line), that is applied for time $t_\pi = \pi/\Omega_1$. The pulse period is $\tau = 0.2$ and the detuning is $\Delta_1 = 0$ (top) and $\Delta_1 = 3$ (bottom).

is due to a driving field with Rabi frequency $\Omega_1 = 50$ that is applied for time $t_\pi = \pi/\Omega_1$. The figure shows results for inter-pulse delays, $\tau = 0.1$ (black solid line), $\tau = 0.2$ (dashed blue line), $\tau = 0.3$ (dashed green line), $\tau = 0.4$ (dotted red line). The spectrum features two symmetric main peaks separated by a frequency π/τ with a clear similarity with the Autler-Townes splitting obtained for a continuous resonant drive [19, 24, 25]. Note that there are additional peaks centered around frequencies that are integer multiples of $\pm\pi/2\tau$ but with exponentially suppressed spectral weights. These additional peaks with smaller spectral weight are visible in the figure for large τ values.

Next, we examine the dependence of this $|2\rangle \leftrightarrow |3\rangle$ absorption spectrum on the Rabi frequency of the pulses. This is equivalent to examining how this spectrum varies with the duration of the π pulses. Fig. 4 shows this absorption spectrum for a pulse period $\tau = 0.2$ for $\Delta_1 = 0$ (top) and $\Delta_1 = 3$ (bottom) for pulse Rabi frequency

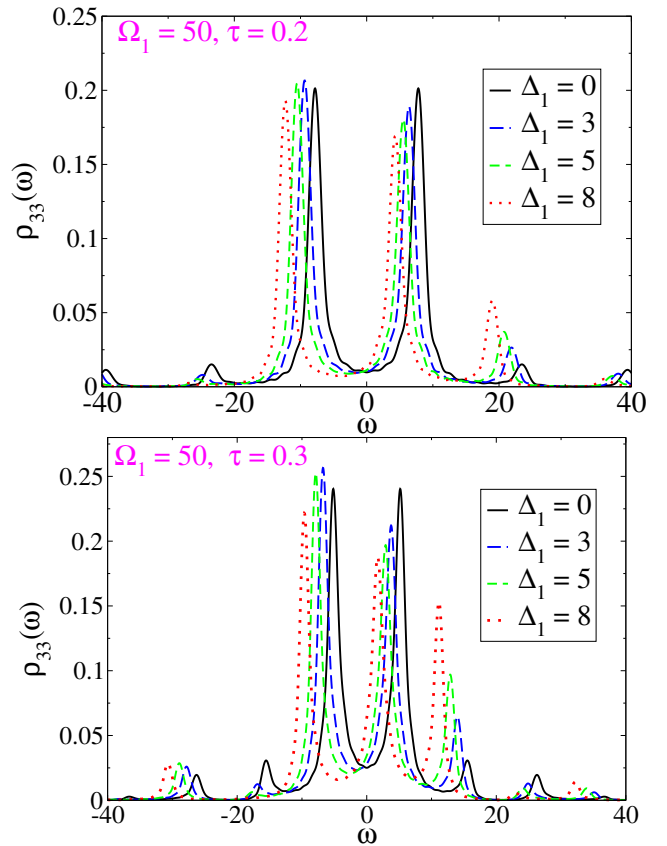


FIG. 5. Population of the second excited state or absorption spectrum of the ($|2\rangle \leftrightarrow |3\rangle$) transition when the ($|1\rangle \leftrightarrow |2\rangle$) is driven by a periodic sequence of π pulses with period $\tau = 0.2$ (top) and $\tau = 0.3$ (bottom). The π pulses are achieved with Rabi frequency $\Omega_1 = 50$. The detuning with the pulse carrier frequency is $\Delta_1 = 0$ (solid black line), $\Delta_1 = 3$ (dashed blue line), $\Delta_1 = 5$ (dashed green line), $\Delta_1 = 8$ (dotted red line).

$\Omega_1 = 100$ (solid black line), $\Omega_1 = 50$ (solid red line), $\Omega_1 = 25$ (dashed blue line). One readily observes a weak dependence on the Rabi frequency. The lineshape is preserved even for relatively broad pulses ($t_\pi \sim \tau/2$). For finite detuning, we observe an asymmetry in the absorption spectrum and with more spectral weight shifted to the satellite peaks. This feature is emphasized in Fig. 5 that shows the absorption spectrum for different detunings. Here, $\tau = 0.2$ (top panel) and $\tau = 0.3$ (bottom panel). The π pulses are achieved by a driving field with Rabi frequency $\Omega_1 = 50$. The detuning with the pulse carrier frequency is $\Delta_1 = 0$ (solid black line), $\Delta_1 = 3$ (dashed blue line), $\Delta_1 = 5$ (dashed green line), $\Delta_1 = 8$ (dotted red line). Here, we observe the shift in the location of the peaks and their relative amplitudes as a function of the detuning with more pronounced asymmetry found in the results for larger inter-pulse delay.

IV. CONCLUSION

The Autler-Townes effect and its parent phenomenon, electromagnetically induced transparency, have been actively investigated since their discoveries. Their applications have been demonstrated in recent advances as quantum memories in quantum information processing. The Autler-Townes effect is readily explained by the dressed state picture that is also responsible for the Mollow triplet of resonance fluorescence occurring when a two-level system is driven on resonance by a strong incident field. Previous work has shown that when a two-level system is instead driven by a periodic sequence of π pulses, the emission spectrum obtained has similarities with the Mollow triplet. This spectrum features a central peak at the pulse carrier frequency and two satellite peaks at $\pm\pi/\tau$ where τ is the inter-pulse delay of the sequence. In the present paper, we have evaluated, the absorption spectrum of the three-level system in the ladder configuration when the bottom two levels are driven by a periodic sequence of π pulses, while the transition

between the middle and the highest level is probed by a weak field. For a pulse carrier frequency that is resonant with the transition frequency of the bottom two levels, this absorption spectrum displays similarities with the Autler-Townes doublet. It features two main peaks at frequencies separated by π/τ . This spectrum is found to have little dependence on the pulse carrier frequency and shows little change even for rather broad pulses (pulse duration $\sim \tau/2$). For finite detuning, the spectrum has an asymmetry that increases with the detuning. These results demonstrate the capacity to modulate the absorption spectrum of a three-level system with experimentally achievable pulse protocols and provide an alternative pathway for realizing quantum memories in these systems.

ACKNOWLEDGMENT

We acknowledge support from the National Science Foundation under Grants No. PHY-2014023 and No. QIS-2328752.

-
- [1] B. R. Mollow, Power spectrum of light scattered by two-level systems, *Phys. Rev.* **188**, 1969 (1969).
- [2] B. R. Mollow, Stimulated emission and absorption near resonance for driven systems, *Phys. Rev. A* **5**, 2217 (1972).
- [3] C. Cohen-Tannoudji, J. Dupont-Roc, and G. Grynberg, *Atom-Photon Interactions, Basic Processes and Applications* (John Wiley & Sons, Inc., New York, 1992).
- [4] H. F. Fotso, A. E. Feiguin, D. D. Awschalom, and V. V. Dobrovitski, Suppressing spectral diffusion of emitted photons with optical pulses, *Phys. Rev. Lett.* **116**, 033603 (2016).
- [5] H. F. Fotso, Controlling the emission and absorption spectrum of a quantum emitter in a dynamic environment, *Journal of Physics B: Atomic, Molecular and Optical Physics* **52**, 025501 (2018).
- [6] D. M. Lukin, A. D. White, R. Trivedi, M. A. Guidry, N. Morioka, C. Babin, Ö. O. Soykal, J. Ul-Hassan, N. T. Son, T. Ohshima, P. K. Vasireddy, M. H. Nasr, S. Sun, J.-P. W. MacLean, C. Dory, E. A. Nanni, J. Wrachtrup, F. Kaiser, and J. Vučković, Spectrally reconfigurable quantum emitters enabled by optimized fast modulation, *npj Quantum Information* **6**, 80 (2020).
- [7] A. G. Campos, D. I. Bondar, R. Cabrera, and H. A. Rabitz, How to make distinct dynamical systems appear spectrally identical, *Phys. Rev. Lett.* **118**, 083201 (2017).
- [8] H. F. Fotso, Pulse-enhanced two-photon interference with solid state quantum emitters, *Phys. Rev. B* **100**, 094309 (2019).
- [9] H. F. Fotso, Tuning spectral properties of individual and multiple quantum emitters in noisy environments, *Phys. Rev. A* **107**, 023719 (2023).
- [10] H. F. Fotso and V. V. Dobrovitski, Absorption spectrum of a two-level system subjected to a periodic pulse sequence, *Phys. Rev. B* **95**, 214301 (2017).
- [11] T. Joas, A. M. Waeber, G. Braunbeck, and F. Reinhard, Quantum sensing of weak radio-frequency signals by pulsed mollow absorption spectroscopy, *Nature Communications* **8**, 964 (2017).
- [12] S. E. Harris, Electromagnetically induced transparency, *Physics Today* **50**, 36 (1997), https://pubs.aip.org/physicstoday/article-pdf/50/7/36/8312202/36_1_online.pdf.
- [13] K.-J. Boller, A. Imamoglu, and S. E. Harris, Observation of electromagnetically induced transparency, *Phys. Rev. Lett.* **66**, 2593 (1991).
- [14] M. Fleischhauer, A. Imamoglu, and J. P. Marangos, Electromagnetically induced transparency: Optics in coherent media, *Rev. Mod. Phys.* **77**, 633 (2005).
- [15] M. Bajcsy, A. S. Zibrov, and M. D. Lukin, Stationary pulses of light in an atomic medium, *Nature* **426**, 638 (2003).
- [16] M. Fleischhauer and M. D. Lukin, Dark-state polaritons in electromagnetically induced transparency, *Phys. Rev. Lett.* **84**, 5094 (2000).
- [17] J. Appel, E. Figueroa, D. Korystov, M. Lobino, and A. I. Lvovsky, Quantum memory for squeezed light, *Phys. Rev. Lett.* **100**, 093602 (2008).
- [18] D. Schraft, M. Hain, N. Lorenz, and T. Halfmann, Stopped light at high storage efficiency in a $\text{pr}^{3+} : \text{y}_2\text{si}_5\text{o}_5$ crystal, *Phys. Rev. Lett.* **116**, 073602 (2016).
- [19] S. H. Autler and C. H. Townes, Stark effect in rapidly varying fields, *Phys. Rev.* **100**, 703 (1955).
- [20] X. He, P. T. H. Fisk, and N. B. Manson, Autler-townes effect of the photoexcited diamond nitrogen-vacancy center in its triplet ground state, *Journal of Applied Physics* **72**, 211 (1992), https://pubs.aip.org/aip/jap/article-pdf/72/1/211/18651173/211_1_online.pdf.
- [21] J. L. Picque and J. Pinard, Direct observation of the autler-townes effect in the optical range, *Journal of*

- Physics B: Atomic and Molecular Physics **9**, L77 (1976).
- [22] E. Saglamyurek, T. Hrushevskyi, A. Rastogi, K. Heshami, and L. J. LeBlanc, Coherent storage and manipulation of broadband photons via dynamically controlled autler–townes splitting, *Nature Photonics* **12**, 774 (2018).
- [23] A. Rastogi, E. Saglamyurek, T. Hrushevskyi, S. Hubele, and L. J. LeBlanc, Discerning quantum memories based on electromagnetically-induced-transparency and autler–townes-splitting protocols, *Phys. Rev. A* **100**, 012314 (2019).
- [24] P. Knight and P. Milonni, The rabi frequency in optical spectra, *Physics Reports* **66**, 21 (1980).
- [25] C. Delsart and J. C. Keller, Observation of the optical autler-townes splitting in neon gas with a cascade level scheme, *Journal of Physics B: Atomic and Molecular Physics* **9**, 2769 (1976).